MOLECULAR MOBILITY AND GAS TRANSPORT PROPERTIES OF POLYCARBONATE-BASED NANOCOMPOSITES

M. Böhning, H. Goering, N. Hao, R. Mach, F. Oleszak and A. Schönhals

Bundesanstalt für Materialforschung und –prüfung (BAM), Unter den Eichen 87, D-12205 Berlin, Germany

Abstract. Plasma synthesized SiC nanoparticles are dispersed in dichloromethane/ poly(bisphenol-A-carbonate) (PC) solutions by high power ultrasonification. The nanoparticle dispersion is stabilized during film casting under well adapted preparation conditions.

The influence of the SiC nanoparticles on the molecular mobility of the PC is studied by dielectric relaxation spectroscopy using films of about 50 µm thickness. No effect on the cooperative segmental mobility (glass transition) is detected. But the relaxation region corresponding to localised fluctuations is strongly broadened and the activation energy is reduced with increasing nanoparticle concentration. The most significant change is observed in the relaxation region between α- and β-process. Corresponding gas transport properties of these nanocomposite films are characterized in terms of permeability, diffusivity and solubility. Results can be interpreted based on an altered local free volume distribution and a change of molecular mobility of the polymer matrix near the nanoparticle surface. Concentration dependent CO_2 permeation experiments reveal a significant reduction of plasticisation effects in the nanocomposites compared to the pure PC film.

1. INTRODUCTION

In recent years polymer based nanocomposite materials gained a steadily growing interest in science as well as in industry due to their unique physical properties and property combinations. The small size of the filler particles incorporated in polymeric matrix materials results in remarkable features, especially concerning optical properties (e.g. transparency) and the amount of interface area in such nanocomposites, combined with desired modifications, such as electrical, mechanical or barrier properties as well as fire-retardancy.

Because of the large amount of interface area (resulting from the high surface to volume ratio of the nanosize filler particles) the influence of the interphase, i.e. the part of the polymeric matrix which is directly influenced by an adjacent nanoparticle surface, can play a decisive role for the performance of the nanocomposite material, especially for the transport of small penetrant molecules (gases or vapours).

Furthermore the length-scale of interaction between filler particle and polymeric matrix, which may be considerably smaller than in conventional composite materials, leads to modifications in packing structure and dynamics of the polymer. Resulting subtle changes in the free volume distribution can give rise to unusual properties. For example with respect to gas transport behaviour of such materials an unexpected increase in permeability for small penetrant molecules (methane) for membranes of glassy nanocomposite materials based on poly(4-methyl-2-pentyne) (PMP) filled with nanoscale fumed silica particles combined with an unusual permselectivity for large organic molecules over small permanent gases has been reported by Merkel *et al.* [1].

Corresponding author: M. Böhning, e-mail: Martin.Boehning@bam.de

A combination of dielectric relaxation spectroscopy (DRS) with systematic investigations of gas transport properties was chosen in order to reveal structural changes as well as dynamic behaviour of polymer based nanocomposite materials.

Dielectric relaxation spectroscopy (DRS). DRS is a useful tool to study the molecular dynamics of polymeric systems [2]. This method provides direct information about the molecular dynamics of dipole moments related to the polymer chain or parts of it. Moreover, the results can be taken as a probe for structural features as motional processes of dipoles depend on their local environment and therefore reveal information on micromorphology of the system under investigation. The complex dielectric function

$$\varepsilon^*(f) = \varepsilon'(f) - i \cdot \varepsilon''(f), \quad (i = \sqrt{-1}) \qquad (1)$$

characterises the dielectric properties of a material. If the frequency f of the applied electric field corresponds to reorientation times of molecular dipoles $\varepsilon^*(f)$ shows a characteristic pattern. The real part $\varepsilon'(f)$ decreases step-like with increasing frequency, whereas dielectric loss or imaginary $\varepsilon''(f)$ exhibits a maximum. From the frequency of maximal loss f_p the relaxation rate of the fluctuating dipoles can be estimated. For details see [2].

Gas transport properties in the polymeric matrix. The transport of small penetrant molecules through nonporous amorphous polymer layers is generally described on the basis of the solution-diffusion mechanism. The driving force is the concentration gradient across the membrane layer due to a pressure difference between its upstream and downstream side. The overall transport, characterised by the permeability coefficient P, is the result of three steps: (1) the sorption of penetrant molecules at the upstream side (described by the solubility coefficient S), (2) the diffusive transport across the membrane layer (diffusion coefficient D) and (3) the desorption at the downsteam side. Accordingly the permeability coefficient is the product of D and S, see Eq. (2).

$$P = D \cdot S. \qquad (2)$$

The gas transport in glassy polymers is usually interpreted in terms of the *Dual Mode Sorption*-model (Eq. (3)) [3, 4] describing the sorbed penetrant concentration C as the sum of a Henry-type solubility (C_D) and a Langmuir-type sorption (C_H) resulting in sorption isotherms exhibiting a characteristic decrease of solubility S and decreasing permeability P with increasing pressure/concentration.

$$C = C_D + C_H = k_D \cdot p + \frac{C_H' b p}{1 + bp}, \qquad (3)$$

(k_D: Henry coefficient, C_H': Langmuir capacity, b: Langmuir hole affinity constant).

For highly sorbing gases (e.g. CO_2) and vapours often a plasticisation of the polymeric matrix is observed leading to an increase of P and S above a plasticisation pressure p^*. This is often connected with a significant loss in permselectivity and mechanical stability. Therefore several attempts have been made to suppress plasticisation in such systems [5-7].

2. MATERIALS

Plasma synthesis of SiC nanopowder. The SiC nanopowders were synthesized via gas phase condensation reactions by a thermal RF induction plasma at atmospheric pressure. The custom-made RF induction plasma torch used is of standard design with a quartz plasma confinement tube. The plasma was generated in an argon/hydrogen mixture (10% H_2) at a plate power of 30 kW. Silicon tetrachloride was diluted with H_2-carrier gas, and directly injected into the plasma tail. Reactive quenching with C_2H_4 as carburising agent was applied. The produced SiC nanopowders were collected in an electrical filter where the particles were charged and separated by a negative wire corona.

TEM analysis of the nanopowder revealed a size distribution between 20 and 60 nm for the primary particles and the occurrence of frog spawn like agglomerates (length: 200 to 500 nm). The primary particles consist of a crystalline SiC core and an amorphous outer shell. Carbon species are also formed during the reaction.

Preparation of nanocomposite films. Nanocomposites were prepared from solution using poly (bisphenol-A carbonate) (PC, Sigma-Aldrich) as matrix polymer and the SiC nanoparticles as filler. The SiC nanopowder, described above, was dispersed in a 4.5 weight-% solution of PC in dichloromethane by 5 minutes ultrasonification (Bandelin Sonopuls HD200/UW200 homogeniser with KE76 titanium tapered tip, pulsed mode). The dispersion was cast into a petri dish and during the first stage of evaporation of the solvent at room temperature the atmosphere (air/nitrogen / dichloro-methane vapor) was controlled to get fully amorphous films and to minimize the sedimentation of the nanoparticles. Subsequently the films were further dried at 90 °C in a vacuum oven for 24 h resulting in samples of
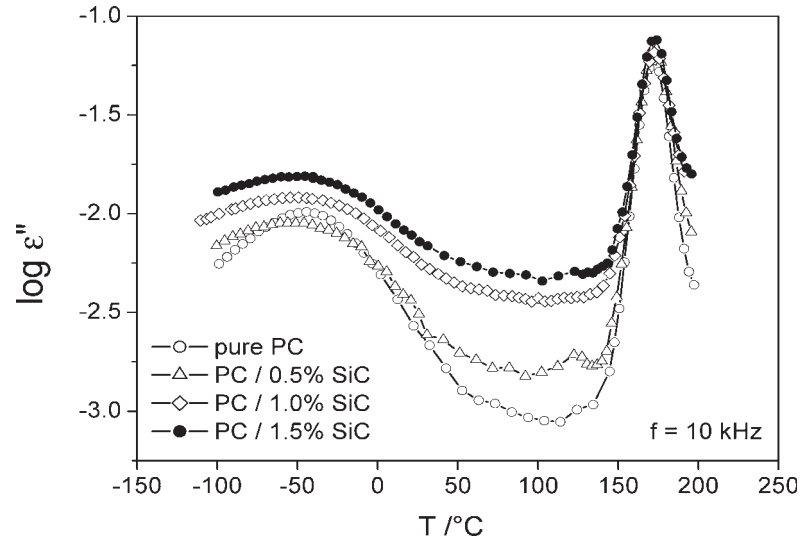
Fig. 1. Dielectric loss vs. temperature at 10 kHz of PC and PC/SiC-nanocomposite films.

about 50 µm thickness. The SiC concentration was varied from 0.5 wt.% to 5.0 wt.%.

3. EXPERIMENTAL

Dielectric relaxation spectroscopy. Details of the procedure for the dielectric measurements have been described elsewhere (see Chapter 2 in [2]). Samples (20 mm diameter; thickness of about 50 µm) were placed between gold-plated stainless steel electrodes. $\varepsilon^*(f)$ was measured in the frequency range from 0.1 to 10^6 Hz by a frequency response analyser Schlumberger FRA 1260 coupled to a buffer amplifier of variable gain (Chelsea Dielectric Interface). The temperature of the sample T was controlled by a custom-made gas jet heating system operated with liquid nitrogen. The sample was thermally equilibrated at the selected temperatures with an accuracy of 0.05K.

Gas permeation. Permeation experiments were performed in the upstream pressure range from 1.0 to 20 bar based on the time-lag method [4] using a temperature controlled set-up. The samples were degassed prior to measurements. The pressure increase in the closed downstream volume (p_2) was determined by a Baratron gauge. The films had a diameter of 40 mm and a thickness between 40 and 70 µm. The permeability P is calculated from the linear pressure increase in the steady state region of the curve (Eq. (4))

$$P = \frac{V l T_0}{A T p_1 p_0}\left(\frac{dp_2}{dt}\right)_s,$$ (4)

(V: downstream volume, l: membrane thickness, $T_0 = 273.15$K, A: membrane area, p_1: upstream pressure, $p_0 = 1.013$ bar, $(dp_2/dt)_s$: steady state downstream pressure increase).

Permeability coefficients are given in Barrer:

$$1[Barrer] = 10^{-10}\left[\frac{cm^3(STP)\cdot cm}{cm^2\cdot cmHg\cdot s}\right].$$ The extrapolation of this line to $p_2 = 0$ gives the time-lag τ characterising the initial transient part of the curve. The effective diffusion coefficient D_{eff} is calculated according to

$$D_{eff} = \frac{l^2}{6\tau}.$$ (5)

Gas sorption. Gas sorption was measured gravimetrically using an electronic high pressure microbalance (Sartorius 4406) placed in a temperature controlled air-bath and also equipped with a turbomolecular vacuum pump for degassing. Sorption isotherms are determined from the sum of mass uptakes in successive steps of pressure increase in the system. The kinetic of individual mass uptake curves allows furthermore the calculation of diffusion coefficients [8].

4. RESULTS AND DISCUSSION

TEM pictures of the nanocomposite films reveal the same structure of the SiC particles as found in the nanopowders. Therefore the particles are well dispersed and properly embedded in the polymeric
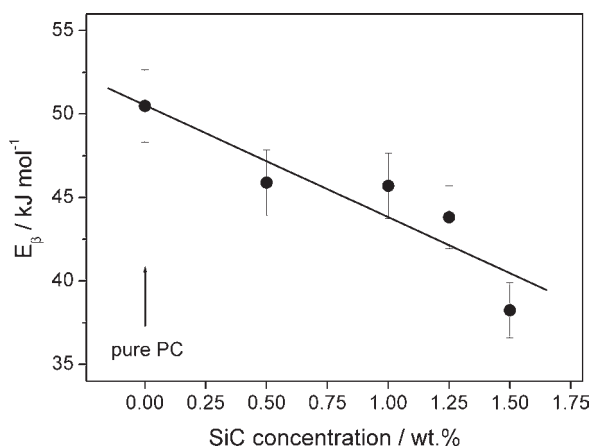
Fig. 2. Activation energy of the β-relaxation E_β as function of SiC nanoparticle concentration in the nanocomposite films.

matrix but the agglomerates formed during particle formation in the thermal plasma process are not destroyed by the ultrasonic treatment.

The dielectric spectra (ε" vs. temperature at f=10 kHz, Fig. 1) of the pure PC as well as the nanocomposite materials show a prominent relaxation peak at 169 °C which has to be assigned to the α-relaxation connected to the glass transition. Furthermore a broad β-relaxation can be identified in the low temperature region (around –40 °C). A comparison of the dielectric spectra of the nanocomposite films with SiC contents of 0.5, 1.0 and 1.5 wt.% with the pure PC film shows a significant broadening of the β-relaxation peak at the low temperature side and also a slight shift to lower temperatures while the α-relaxation remains unchanged. Additionally the dielectric loss in the temperature region between 20 °C and 120 °C increases remarkably.

The β-relaxation is analysed quantitatively and the relaxation rate $f_{p\beta}$ is determined. The temperature dependence of $f_{p\beta}$ can be described by an Arrhenius equation from which the activation energy E_β is estimated. With increasing concentration of the SiC nanoparticles E_β decreases systematically (see Fig. 2). This means that the nanoparticles increase the molecular mobility of these localized fluctuations which must belong to parts of the polymer chain situated close to these nanoparticles. So a boundary layer around a nanoparticle is formed having a higher molecular mobility for localized fluctuations than the bulk. Also the broadening of the β-peak can be understood on this basis. Within the sample there are bulk-like regions – because the concentration of the nanoparticles is low – and regions belonging to the boundary layer. The observed β-peak is just a superposition of these two contributions and therefore the estimated activation energy is an effective one.

It is well accepted that the β-relaxation corresponds to localised fluctuations whereas the α-process is due to the cooperative segmental dynamics (dynamic glass transition). From the general point of view according to the fluctuation-dissipation theorem a finite value of ε" (not only the peak) corresponds to motional processes (for details see Chapter 1 in [2]). Therefore the region in the dielectric spectrum in between the β- and α-process has to be assigned to molecular fluctuations taking place on a length scale between localised and cooperative fluctuations. The dielectric loss in this region increases significantly with the concentration of the nanoparticles (see Fig. 1). This means the nanoparticles increase also the molecular mobility of modes taking place on a larger length scale than the β-process. In general an increase in molecular mobility can be interpreted as an increase in local free volume. So it can be concluded that the nanoparticles modify the local free volume but on a scale which is not large enough to have an impact on the glass transition.

These findings are in agreement with the analysis of gas sorption isotherms in the framework of the *Dual Mode Sorption*-model. A significant change in the shape of the sorption isotherms of CO_2 at 35 °C (up to 50 bar) can be observed which is clearly reflected by the *Dual Mode* parameters determined by curve fitting (see Table 1). Hole affinity constant (b) and Langmuir capacity ($C_H^{'}$) are reduced in the nanocomposite materials compared to the pure PC whereas the Henry coefficient (k_D) is remarkably increased. This reflects a higher fraction of highly fluctuating free volume (corresponding to the Henry sorption mode) in the nanocomposites due to a modified local free volume distribution and a higher molecular mobility in the vicinity of the embedded SiC nanoparticles.

Table 1. *Dual Mode Sorption*-parameters of the sorption isotherms of CO_2 measured at 35 °C in the pressure range between 1 and 50 bar. Units: [k_D] = 1cm³(STP)/(cm³(polymer) bar); [b]=1 bar⁻¹, [$C_H^{'}$]=1 cm³(STP)/cm³(polymer).

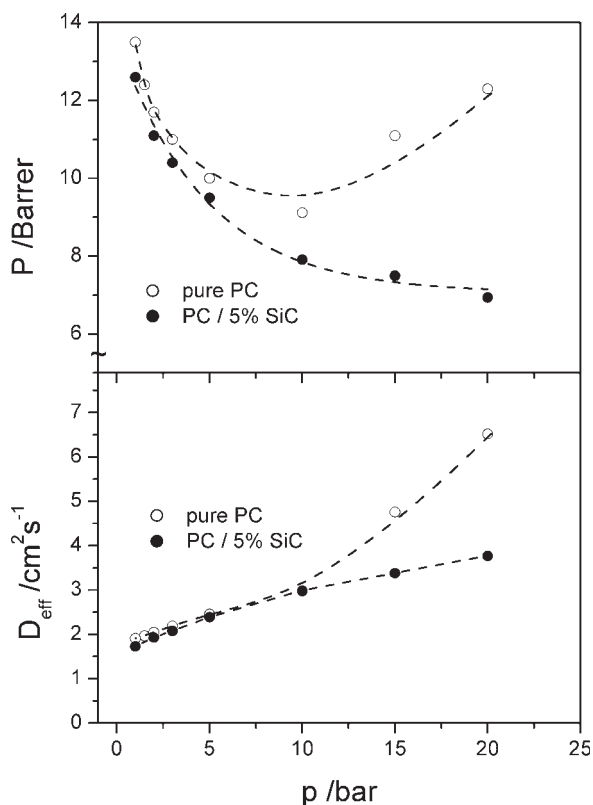| Sample	k_D	b	$C_H^{'}$
pure PC	0.27	0.33	15.2
PC/1.5 wt.% SiC	0.53	0.14	13.6
PC/5.0 wt.%SiC	0.57	0.13	13.9

Fig. 3. Pressure dependent permeability coefficient *P* and diffusion coefficient D_{eff} of CO_2 in pure PC and the nanocomposite film containing 5.0 wt.% SiC.

Pressure dependent permeation experiments (CO_2 at 35 °C, Fig. 3) reveal a significant tendency of plasticisation of the pure PC film under investigation, i.e. an increase of the permeability coefficient in the pressure region above 10 bar. Below this plasticisation pressure the characteristic *Dual Mode*-behaviour (decreasing *P*) is observed. Corresponding diffusion coefficients also strongly increase above 10 bar. In contrast the nanocomposite film containing 5.0 wt.% SiC does not exhibit this plasticisation behaviour.

As the overall level of permeability remains nearly unchanged the introduction of nanoparticles into a polymeric matrix may be the basis for a possible route to obtain polymer based membrane materials with improved performance due to suppressed plasticisation phenomena.

ACKNOWLEDGEMENTS

REFERENCES

[1] T. C. Merkel, B. D. Freeman, R. J. Spontak, Z. He, I. Pinnau, P. Meakin and A. J. Hill // *Science* **296** (2002) 519.
[2] F. Kremer, A. Schönhals, *Broadband Dielectric Spectroscopy* (Springer, Berlin, 2002).
[3] D.R. Paul // *Ber. Bunsenges. Phys. Chem.* **83** (1979) 294.
[4] J.H. Petropoulos, In: *Polymeric Gas Separation Membranes*, ed. by D.R. Paul and Y.U. Yampol'skii (CRC Press: Boca Raton, 1994) p.17ff.
[5] A.F. Ismail and W. Lorna // *Sep. Purif. Technol.* **27** (2002) 173.
[6] A. Bos, I.G.M. Pünt, M. Wessling and H. Strathmann // *J. Membrane Sci.* **155** (1999) 67.
[7] A. Bos, I. G. M. Pünt, M. Wessling and H. Strathmann // *J. Polym. Sci.: Part B: Polym. Phys.* **36** (1998) 1547.
[8] J. Crank, *The Mathematics of Diffusion* (Oxford University Press, Oxford, 1975).